Miner Deposita (2017) 52:181–196
DOI 10.1007/s00126-016-0658-8

ARTICLE

The Kohuamuri siliceous sinter as a vector for epithermal mineralisation, Coromandel Volcanic Zone, New Zealand

Ayrton Hamilton[1] · **Kathleen Campbell**[1] · **Julie Rowland**[1] · **Patrick Browne**[2]

Received: 29 June 2015 / Accepted: 7 April 2016 / Published online: 19 April 2016

Abstract The Kohuamuri siliceous sinter is the largest known fossil hot-spring system in the Hauraki Goldfield, a 200 × 40 km volcanic terrain with at least 50 adularia-illite epithermal deposits formed 16.3–5.6 Ma within the Coromandel Volcanic Zone, New Zealand. The sinter is associated with rhyolite and ignimbrite of the Whitianga Caldera (Miocene–Pliocene) and consists of two deposits, the Kohuamuri deposit itself, a large in situ outcrop (47,000 m^2) and its associated sinter boulder field (4500 m^2), and the Kaitoke deposit 900 m to the southwest, comprising boulders in a landslide situated on a normal fault. The well-preserved macroscopic and microscopic textures at Kohuamuri are similar to actively forming and ancient hot-spring deposits elsewhere, derived from deep circulating, magmatically heated, near-neutral pH alkali chloride fluids oversaturated in amorphous silica and that discharge at the Earth's surface at ≤100 °C. Lithofacies, petrography, mineralogy, as well as trace element concentrations of the Kohuamuri/Kaitoke deposits were used to locate likely palaeo-thermal conduits from the deep reservoir and to reconstruct the palaeoenvironmental setting of the siliceous sinter as an aid to assessing the economic potential of the ancient geothermal system. Both deposits contain the high-temperature (>75 °C) geyserite lithofacies, with the Kohuamuri deposit also exhibiting textures affiliated with cooler middle and distal sinter apron areas, as well as geothermally influenced marsh facies. Trace element analysis of sinter lithofacies revealed concentrations and zonations of Au, Ag, base metals (Pb, Cu, Zn) and pathfinder elements (As, Sb) associated with epithermal deposits, elevated in the proximal vent area, and providing evidence of possible Au and Ag ore mineralisation at depth. The methodology used in this study could be utilised globally to identify and assess as yet unidentified epithermal deposits.

Keywords Siliceous sinter · Epithermal · Mineralisation vector · Hauraki goldfield · Palaeoenvironmental reconstruction · Coromandel Volcanic Zone · New Zealand

Editorial handling: H. Frimmel

Electronic supplementary material The online version of this article (doi:10.1007/s00126-016-0658-8) contains supplementary material, which is available to authorized users.

✉ Kathleen Campbell
ka.campbell@auckland.ac.nz

[1] Geology, School of Environment, University of Auckland, Private Bag 92019, Auckland 1142, New Zealand

[2] Institute of Earth Sciences and Engineering, University of Auckland, Private Bag 92019, Auckland, New Zealand

Introduction

Siliceous sinters are surface expressions of epithermal systems in which fluids derived from deep reservoirs with temperatures >175 °C are discharged at the Earth's surface (Fournier and Rowe 1966). Upon cooling, these fluids deposit non-crystalline opal-A that precipitates onto biotic and abiotic surfaces to form erosion-resistant sinter mounds and sheet deposits, metres to tens of metres thick (Fournier and Rowe 1966; Fournier 1985; Lynne et al. 2008; Guido and Campbell 2011; Lynne 2012). Sinter deposits are geothermal features that form where hot fluids are expelled at the intersection of the water table with the Earth's surface (Sillitoe and Hedenquist 2003; Simmons et al. 2005), typically above or adjacent to epithermal deposits occurring at shallow depths in the Earth's crust (Sillitoe 2015). The geographic area occupied by a given sinter deposit is typically small in comparison to the often extensive lateral and vertical footprint of epithermal

mineralisation (e.g. veins, regional late silicification), and therefore sinters provide precise information about the depth level of exposure of a palaeo-epithermal system. Because vent areas in particular represent conduits of fluid flow from the reservoir to the surface, they help pinpoint where epithermal mineralisation is most likely to be found. Indeed, siliceous sinter deposits have been shown to have potential as reliable vectors for epithermal mineralisation at shallow depths in mining districts elsewhere (Buchanan 1981; White et al. 1989; Sherlock et al. 1995; Guido and Campbell 2011, 2014; Lynne 2012). For example, at the McLaughlin Mine in California, USA, exposed Quaternary sinter was the only surface expression of a bonanza deposit (Sherlock et al. 1995). The textures, mineralogy, petrography and chemical composition of sinter deposits may be utilised in palaeoenvironmental and palaeo-hydrological reconstructions of temperature, pH, fluid composition, flow directions and relative discharge volumes of extinct hot-spring systems, from high-temperature (~100–75 °C) vent geyserites to ambient (~25 °C), plant-rich, thermally influenced silicified marsh deposits (Fig. 1) (Fournier and Rowe 1966; Walter 1976; Fournier 1985; Cady and Farmer 1996; Campbell et al. 2001, 2015a, b; Guido and Campbell 2011). This potential hot fluid-conduit link between epithermal deposits and siliceous sinters at the land surface may allow sinters to be used in assessing the mineralisation environment of an epithermal system.

The Kohuamuri sinter is a well-preserved, fossilised, siliceous hot-spring deposit located in the eastern province of the Hauraki Goldfield, hosted in Miocene–Pliocene rocks of the Coromandel Volcanic Zone (CVZ), New Zealand (Fig. 2). The Kohuamuri siliceous sinter is the largest known fossil hot-spring deposit in the region, comprising the Kohuamuri deposit, a large in situ outcrop (47,000 m^2) and its associated sinter boulder field (4500 m^2), and the Kaitoke deposit situated 900 m to the southwest, constituting a landslide-related sinter boulder field (49,000 m^2) located on a normal fault. The Kohuamuri sinter has been of interest in the past for its association with gold mineralisation, with reports of minor amounts of gold being extracted from the sinter in early mining attempts (McKay 1897). In a regional geological study of the Mercury Bay area, Skinner (1995) also recorded the Kohuamuri sinter and briefly described its physical appearance. Within the CVZ, half a dozen sinters are documented (Fig. 2), which were used during early exploration of regional epithermal systems as special indicators, and geochemical analyses were conducted on some sinter deposits (Fraser and Adams 1907; Bell and Fraser 1912). A more recent study (Stevens and Boswell 2006) analysed the Onemana hydrothermal eruption breccia, which contains sinter clasts, and revealed anomalous Au, Ag, As and Sb concentrations. Arsenic and antimony contents reach up to 650 and 114 ppm, respectively, with the highest gold concentrations centred around the inferred vent locality.

This study examines the preserved textures, mineralogy, petrography and elemental concentrations of the Kohuamuri sinter. We compare collected data to modern analogues and other studies to reconstruct the palaeoenvironment and to evaluate its worth as a vector for geothermal fluid flow and mineralisation.

Geologic context

The Kohuamuri sinter is the largest (0.2 km^2) known sinter in the Hauraki Goldfield, a 200 × 40 km region of 50 gold-bearing, adularia-illite type epithermal deposits and several porphyry copper prospects associated with the Coromandel Volcanic Zone, North Island, New Zealand (Fig. 2) (Brathwaite et al. 2001; Christie et al. 2007). The CVZ is a product of Cenozoic volcanism driven by subduction of the Pacific Plate beneath North Island (Australian Plate) since 25 Ma, with subaerial andesite-dacite sequences and late rhyolite overlying a basement of Mesozoic meta-sedimentary sequences (Skinner 1986). This period of volcanism (20–4 Ma) relates to the rotation of the locus of arc magmatism from Northland to Coromandel by ca. 16 Ma, and its southeastward migration from Coromandel to the Taupo Volcanic Zone (TVZ) by 2 Ma (King 2000; Christie et al. 2007; Mauk et al. 2011; Rowland and Simmons 2012; Seebeck et al. 2014).

The CVZ was constructed during the Miocene and Pliocene by the products of three volcanic phases (Christie et al. 2007; Booden et al. 2012). The first is recorded by the widespread Coromandel group (18–3.8 Ma) and constitutes andesite and dacite that formed massive lava flows, breccias, lahars, tuffs, dykes and tonalite plutons. The second phase is encompassed by the Whitianga group (9.1–6 Ma), consisting of rhyolite produced by lava flows, ignimbrite sheets, dome volcanoes and large silicic calderas. The third phase comprises the localised Mercury Bay basalts (6.0–4.2 Ma), which represent restricted, mostly Strombolian volcanoes and dykes (Skinner 1986; Adams et al. 1994). As noted by Christie et al. (2007), the epithermal deposits of the Hauraki Goldfield are predominantly hosted in the phase I Coromandel group andesite, but gold-producing deposits also occur in phase II Whitianga group rhyolite and meta-sedimentary greywacke. The goldfield produced 320,000 kg Au and 1.5 million kg Ag between 1862 and 2006 from a total land area of approximately 2900 km^2 (Christie et al. 2007). These deposits are controlled by steeply dipping extensional fault arrays (Brathwaite et al. 2001) and accumulated during the Miocene (16–5 Ma). Furthermore, the regional volcanism and epithermal deposits exhibit a punctuated southerly migration over time (Mauk et al. 2011; Rowland and Simmons 2012; Wilson and Rowland 2015).

The Kohuamuri sinter is located within the Whitianga Volcanic Centre, an area of the Whitianga group volcanic rocks, which includes Miocene and Pliocene rhyolite and

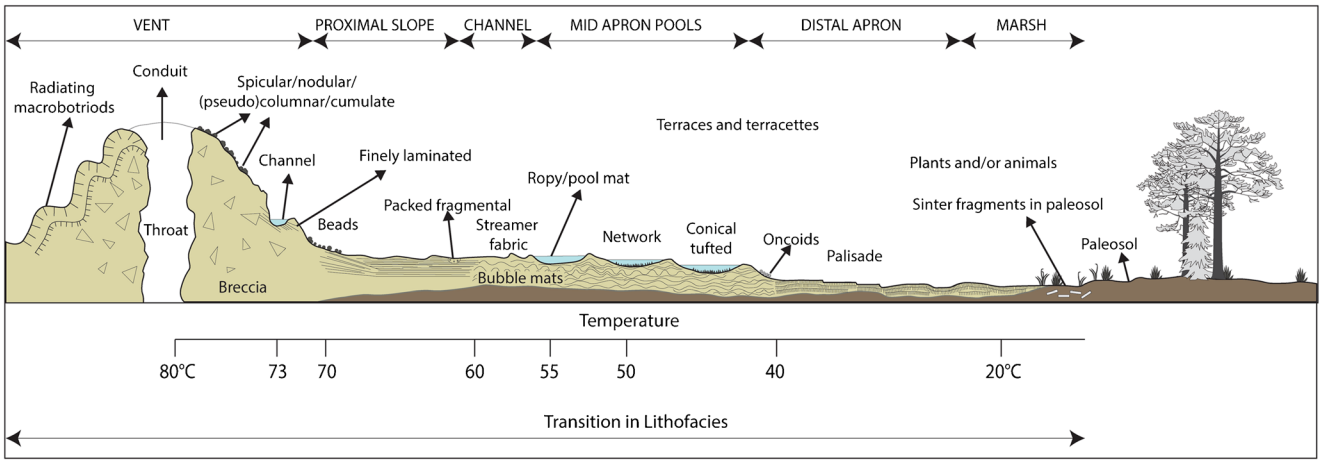

Fig. 1 Schematic cross-section of a siliceous sinter deposit showing the transition of textures associated with a hot-spring discharge temperature gradient (100 °C–ambient), based on facies identified in the Deseado Massif, Argentina, as compared with their analogues in Quaternary to Recent geothermal systems in the Taupo Volcanic Zone (New Zealand) and Yellowstone National Park (Wyoming, USA); modified from Campbell et al. (2015a)

ignimbrite that make up large calderas and stratovolcanoes (Adams et al. 1994). The major feature of the Whitianga Volcanic Centre is the Whitianga caldera (15 km wide × 1–1.5 km deep), as inferred by geophysical data (Briggs et al. 2005; Fig. 2). The in situ Kohuamuri sinter (Fig. 3) is spatially associated with the Pumpkin Rock ignimbrite (5.9 ± 0.7 Ma, Adams et al. 1994), a plagioclase-phyric, pumice-rich, lithic-poor ignimbrite. It overlies the Motutapere rhyolite (7.4 ± 0.85 Ma), a banded and spherulitic rhyolite, and the Flaxmill (7.9 ± 0.1 Ma) rhyolitic dome, a glassy porphyritic rhyolite (Skinner 1995). The volcanic units surrounding the sinter deposits are silicified. Sinter deposition and associated silicification post-date the surrounding volcanic units; therefore, a late Miocene or early Pliocene age is probable (Skinner 1995).

The Kohuamuri deposit (47,000 m^2) is in sharp unconformable contact with the silicified Pumpkin Rock ignimbrite and Motutapere dome (Fig. 3). Kohuamuri Stream intersects the deposit along its northern side to form white sinter bluffs up to 10 m high. The bluffs are highly weathered but contain some original porosity as well as visible centimetre-scale bedding that dips gently <3° west. On the northern side of the stream, an elongated black sinter deposit (~80 × 20 m) is exposed. A boulder field of eroded sinter (boulders up to 2 m^3) lines the southern branch of Kohuamuri Stream, from the in situ deposit to where the stream enters Whitianga Harbour. The Kaitoke deposit is a boulder field situated on a normal fault 900 m southwest of the Kohuamuri deposit and extends over the adjacent Pumpkin Rock ignimbrite (Fig. 3).

Methods

A total of 49 texturally representative sinter samples were collected and analysed from the Kohuamuri sinter (i.e. Kohuamuri and Kaitoke deposits) from 11 locations (7 in situ, 4 ex situ; Fig. 3) in order to map its areal distribution and reconstruct the palaeo-geothermal setting. In general, in modern hot springs, temperature gradients are produced, away from the vent, by the cooling and evaporation of thermal fluids that deposit varied litho- and bio-facies types down the discharge apron (Fig. 1). Sinter textures were examined at macro- and micro-scales using hand sample slab study, transmitted light microscopy of thin sections and scanning electron microscope (SEM) analysis of freshly broken rock chips. For SEM analysis, samples were coated with a thin layer of platinum using a Hitachi E1045 ion sputter coating unit. The coated surfaces were then scanned using a Hitachi SU-70 field emission scanning electron microscope with embedded software and acceleration voltages between 5 and 10 kV. To determine the likely conditions of formation, textural comparisons were made with Quaternary to Recent examples from the TVZ and Yellowstone National Park (YNP), USA, to aid interpretation of the Coromandel samples with respect to their geothermally related palaeoenvironmental gradients.

The bulk mineralogy of eight representative samples was analysed via x-ray diffraction (XRD), following Herdianita et al. (2000), using a Philips PW1050/25 diffractometer with CuKα radiation ($\lambda = 1.5405$) at 40 kV and 20 mA operating conditions, and fitted with a PW 1752 graphite crystal monochronometer. To determine the silica phase maturation state of the deposit, a Witec alphas300 R+ confocal Raman microscope fitted with a Princeton Instruments SP2300 spectrograph with a Nd:YAG laser was used at a 532 μm wavelength at power levels up to 37 mW to scan along 50 μm of selected cut nodules and vugs. Additional minerals were identified using transmitted light microscopy and were compared with other sinters associated with epithermal deposits.

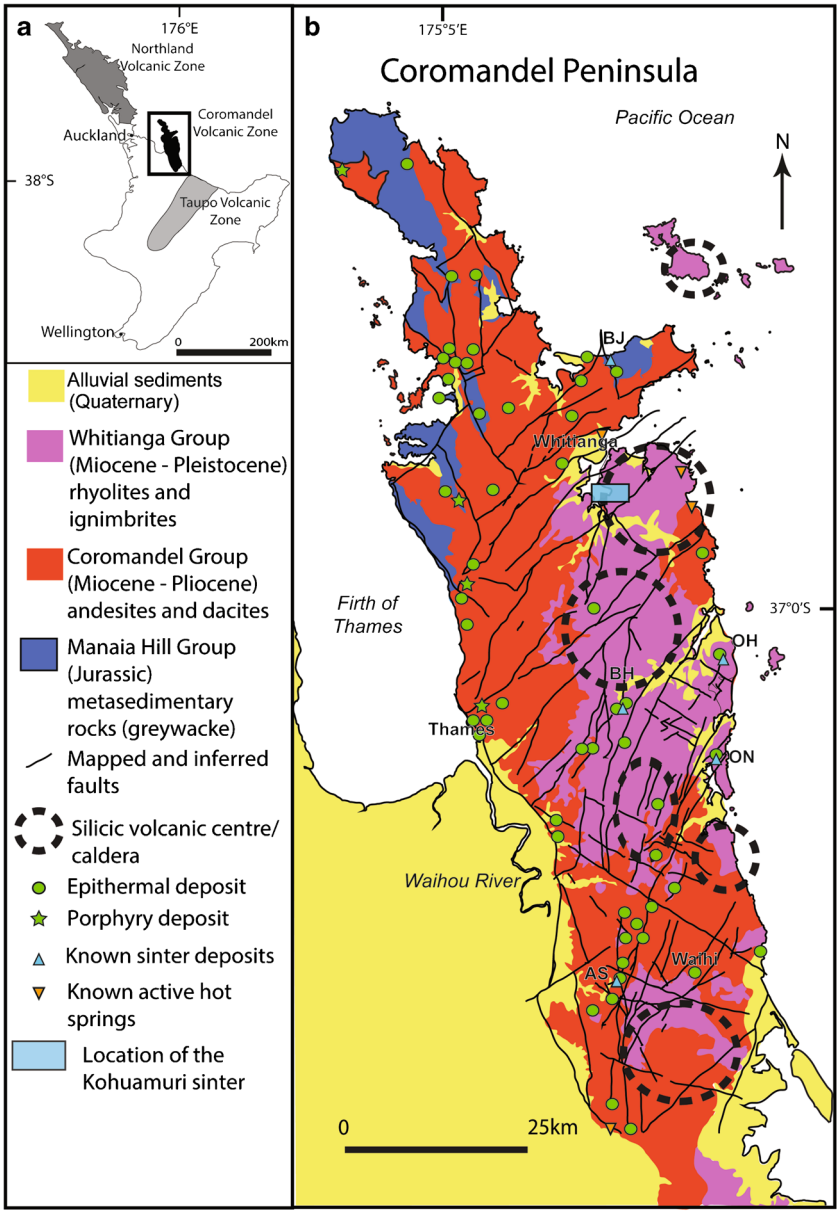

Fig. 2 Geological setting of the Kohuamuri sinter, Coromandel Volcanic Zone (CVZ). **a** Map of North Island, New Zealand, showing location of the CVZ, and the Northland and Taupo volcanic zones. **b** Geological map of the Coromandel Peninsula showing the three major geological groups of the CVZ, mapped major faults, inferred large calderas based on structural and geophysical evidence, and known epithermal, porphyry copper and sinter deposits (*BJ* Blackjack, *OH* Ohui, *ON* Onemana, *AS* Ascot) and active hot springs; location of the Kohuamuri sinter is highlighted by a *blue rectangle*; modified from Skinner (1986), Adams et al. (1994), Rattenbury and Partington (2003) and Christie et al. (2007)

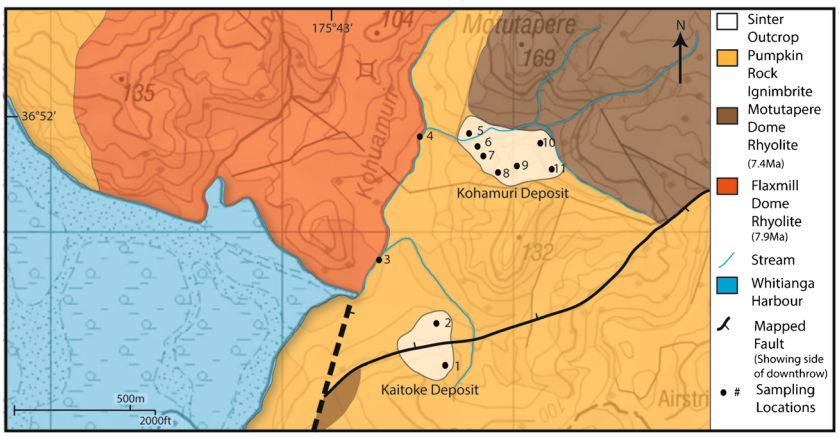

Fig. 3 Geological map of the local Kohuamuri sinter area, comprising the Kohuamuri and Kaitoke deposits, and showing sites (numbered) where sinter samples were collected (Table 1)

To determine trace element concentrations, 18 samples were analysed by Bureau Veritas, New South Wales, Australia, using the Aqua Regia Analysis method. Specifically, 40 g of dried and pulverised sample was dissolved with Aqua Regia in a boiling water bath. An aliquot of this acid was then analysed using atomic absorption spectroscopy (AAS), or inductively coupled plasma mass spectrometry (ICP-MS), to determine their gold contents, with ICP-MS having higher sensitivity than AAS. ICP-MS and inductively coupled plasma atomic emission spectroscopy (ICP-AES) were used to determine the concentrations of the other elements (Ba, Ca, Fe, Mg, Mn, S, Ag, As, Bi, Cu, Hg, Li, Mo, Pb, Sb, Se, Tl, Te, W, Zn).

Results

Textures of the Kohuamuri sinter

Fourteen different palaeoenvironmentally significant textures similar to actively forming sinters from near-neutral pH alkali chloride waters were identified from nine locations associated with the Kohuamuri deposit and two from the Kaitoke deposit. Textures of the Kohuamuri deposit represent an entire geothermal gradient, from high temperature vent and proximal slope areas, through moderate temperature sinter apron pools, to cooler distal apron and thermally influenced marsh settings (Table 1), whereas the Kaitoke deposit only contains textures associated with proximal hot-spring areas.

In detail, several high-temperature (vent to proximal slope facies) sinter fabrics were found in both the Kohuamuri and Kaitoke deposits (Fig. 4). Geyserite with similar textures forms today in spring vent areas (>75 °C) intermittently wetted or splashed by the eruption of geysers to form localised, layered, botryoidal sinter mounds and rims around hot-spring vent pools (Walter 1976; Walter et al. 1996; Braunstein and Lowe 2001; Lowe and Braunstein 2003; Campbell et al. 2015b). At Kohuamuri, vent and proximal slope settings are represented by spicular, nodular and pisoidal ('beaded') geyserite, finely laminated sinter and a silicified, inferred hydrothermal eruption breccia containing clasts of nodular geyserite (Fig. 4). The Kohuamuri hydrothermal breccia contains mixed clasts (sinter, volcaniclastic rocks, hydrothermally altered clasts) with poor sorting (clast size ranges from <5 mm to 10 cm in diameter), in a massive silica matrix (Fig. 4a), similar to the Quaternary Mangatete hydrothermal eruption breccia, TVZ (Fig. 4b; Drake et al. 2014). For example, a clast of nodular geyserite was found in the Kohuamuri hydrothermal eruption breccia (Fig. 4c), akin to nodular geyserite texture forming today at YNP around vent rims (Fig. 4d). Moreover, the Kaitoke deposit contains dense, fine laminae of pisoidal geyserite (Fig. 4e), nearly identical to pisoidal geyserite textures from recently extinct vents (<100 years old) at Geyser Valley, TVZ (Fig. 4f). In addition, spicular geyserite was identified in the Kohuamuri deposit (Fig. 4g), which is similar to spicular geyserite microtextures from present-day sinter (YNP; Fig. 4h). Furthermore, dense, very finely laminated textures develop on proximal vent slopes (~75–90 °C) due to episodically high flow rates that do not allow rapid build-up of sinter (Cady and Farmer 1996; Walter et al. 1996). In the Kohuamuri and Kaitoke deposits, the lamination is composed of white vitreous quartz up to 2 mm thick and laterally continuous for up to 50 cm (Fig. 4i). In places, the layers display small wavelets with amplitudes up to 5 mm and crest distances up to 1 cm apart, inferred as ripples on proximal outflow channel surfaces, similar to textures sampled from geyserite blocks in a steaming landslide deposit at Te Kopia, TVZ (Fig. 4j). At the micro-scale, the size of the microcrystalline quartz crystals within each horizon made it possible to differentiate between individual laminae. This fabric differs from low-temperature distal apron laminated palisade fabric (<40 °C) by its thin and continuous, very regular laminae, and known spatial association with spring-vent areas. The rather thickly laminated palisade fabric bears closely packed, vertical micro-pillars of coarsely filamentous silicified cyanobacteria (Cady and Farmer 1996; Walter et al. 1998; Guido and Campbell 2011; Campbell et al. 2015a). The Kaitoke sinter also has a texture of wavy lamination (2 mm thick), with voids (100 × 50 mm) that are in-filled by siliceous white, brown and dark red sediment in cavities up to 10 mm in diameter. The geopetal fills have an irregular outer morphology that is not parallel to bedding, suggesting the textures represent late stage alteration and dissolution. The red geopetal silicified fill occurs in contact with pisoidal geyserite, so we infer that it formed proximal to a vent.

The Kohuamuri deposit also contains bubble mat, network and conical tufted fabrics (Fig. 5), likely formed in moderate temperature (~40–60 °C), mid-apron pools and discharge channels (Fig. 1). Network fabrics consist of silica threads less than 1 mm thick that are discontinuous in a webbed pattern within stacked horizons (2 cm thick) of bedded sinter. Network fabrics are inferred to form at the drying margins of moderately hot pools, where extracellular polymeric substances (EPS), exuded by cyanobacteria, become dried out and silicified (e.g. Fig. 5b; Guido and Campbell 2011). Bubble mat texture consists of elliptical voids occurring in small, bedding-parallel lenses within wavy laminated to conical tufted sinter (Fig. 5c). In modern-day sinters, bubbles (Fig. 5d) form and become trapped as microbial mats de-gas during photosynthesis (Hinman and Lindstrom 1996), which then become silicified due to the oversaturation of silica in the cooling thermal fluid (Campbell et al. 2001; Guido and Campbell 2011). At Kohuamuri, large fossilised tufts perpendicular to bedding occur as irregularly laminated, cone-shaped features (up to 5 mm wide, 5 cm long) (Fig. 4e). In the present day, conical tufted textures form in mid-apron, terraced pools (e.g. Fig. 5f) via columnar building of pool stromatolites by

Table 1 Facies associations of the Kohuamuri sinter (asterisks (*) indicate that these samples were collected in place)

Facies assemblage	Facies	Textures	Description	Similar occurrences	Site(s)	Inferred formation temperature
Proximal	Vent	Poorly sorted breccia	Matrix-supported angular clasts up to 10 cm in diameter with randomly oriented in silica matrix	Waiotapu, New Zealand (Hedenquist and Henley 1985)	10*	>75 °C
		Nodular geyserite	10 mm in length, 5 mm in width, convex laminae, nodular	Orakei Korako, New Zealand (Lynne 2012)	10*	
		Spicular geyserite	Finely laminated, rounded pillars <0.5 cm tall, 0.2 cm wide	Orakei Korako, Broken Hills, New Zealand (Lynne 2012)	3	
		Geyserite pisoids	Individual pisoids up to 1.5 cm	Orakei Korako, New Zealand (Lynne 2012) Waiketi geyser, Whakarewarewa, New Zealand (Jones et al. 2011)	2	
	Proximal slope	Finely laminated	Alternating siliceous layers <2 mm thick with low amplitude (<1 mm) wavelets	Drummond Basin, Australia (Walter et al. 1996) Umukuri, New Zealand (Campbell et al. 2001)	9*	>60 °C
		Geopetal	Dull red rock containing brown silicified sediment in irregular vugs up to 0.5 cm in diameter		1, 2	
Middle	Mid-apron pools	Network	Highly porous, 1-cm-thick beds containing finely webbed quartz threads	Deseado Massif, Argentina (Guido and Campbell 2011)	11*	40–60 °C
		Lenticular voids	Elliptical voids up to 2 cm in diameter, in lenses	Umukuri, New Zealand (Campbell et al. 2001)	3, 4	
		Conical tufted	Large apical stromatolites that are up to 5 cm tall, 0.4 cm wide	Umukuri, New Zealand (Campbell et al. 2001)	3, 4	
Distal	Distal apron	Palisade	Layers of wavy laminae up to 1 cm thick	Umukuri, New Zealand (Campbell et al. 2001)	3	<40 °C
	Marsh	Plant rich	Silicified plant material and moulds ranging in size up to 10 cm in length and 5 cm in width	Deseado Massif, Argentina (Guido et al. 2010) Umukuri, New Zealand (Campbell et al. 2001)	6*	
		Clotted	Irregular dark fine-grained silica clots	Umukuri, New Zealand (Campbell et al. 2001)	5*	

finely filamentous cyanobacteria (e.g. *Leptolyngbya*) (Walter 1976; Cady and Farmer 1996; Walter et al. 1996; Guido and Campbell 2011; Lynne 2012). At the microscopic scale, these features at Kohuamuri (Fig. 5g) are very similar to conical tufted examples from modern spring pools at Whakarewarewa geothermal area, TVZ (Fig. 5h).

Warm to tepid (<40 °C) distal apron and thermally influenced marsh textures recognised at Kohuamuri included palisade lamination, plant-rich and clotted sinter (Fig. 6). Palisade textures are filamentous structures perpendicular to lamination, in which coarsely filamentous cyanobacterial mats (~0.5–2 mm thick) today produced by the cyanobacterium *Calothrix* are entombed by silica (e.g. Fig. 6a, b) (Cady and Farmer 1996; Lynne 2012; Campbell et al. 2015a). Within the Kohuamuri sinter, palisade fabric was identified as discontinuous, thick, planar to wavy lamination, up to 1 cm thick, containing truncated micro-pillar structures in microcrystalline quartz (Fig. 6a), very similar to Holocene palisade fabric from Orakei Korako, TVZ (Fig. 6b). Moreover, silicified plant material included branches, twigs and reeds without preferential orientation within a very fine-grained quartz matrix (Fig. 6c). Plants become silicified in modern sinters at the cool margins of discharge aprons and in marsh areas (Fig.6d) (Channing et al. 2004). At Kohuamuri, clotted fabric is present in the black sinter on the northern side of Kohuamuri Stream, occurring within very fine-grained quartz with patches of irregular lamination, clots and rare plant material (Fig. 6e, f). In cool, stagnant, marshy margins of modern geothermal areas at YNP, buff coloured, fluffy, clotted microbial encrustations upon plants and sinter fragments are quite

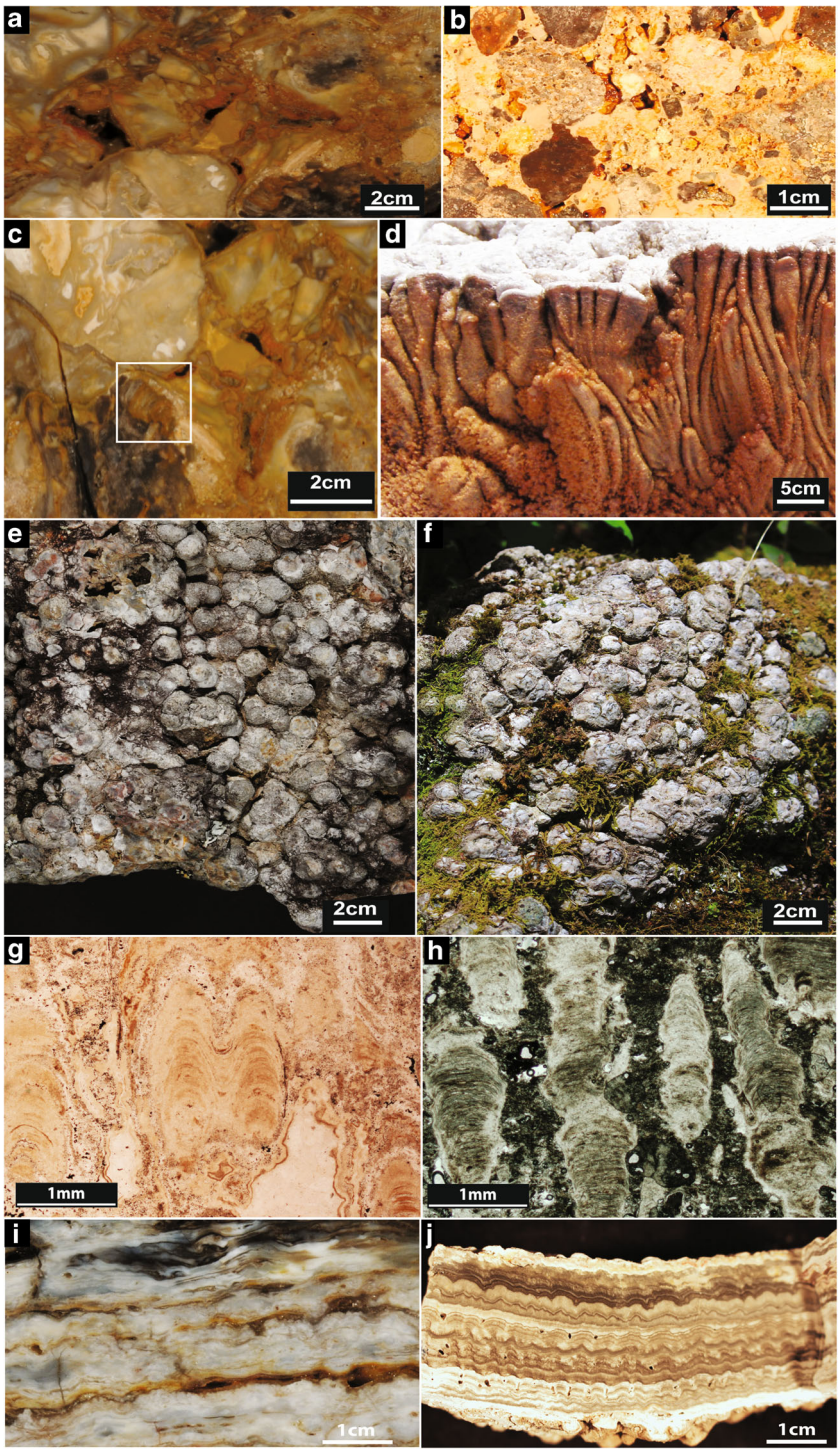

Fig. 4 Vent and proximal facies associations of the Kohuamuri sinter compared to Quaternary analogues. **a** Cut slab of poorly sorted, polymitic clasts of sinter (*black colour*) and volcanic material (*yellow*) in a siliceous matrix; Kohuamuri deposit. **b** Cut slab of hydrothermal breccia from the Quaternary Mangatete sinter, TVZ, showing poorly sorted polymitic clasts in a silica matrix (Drake et al. 2014). **c** Cut slab of poorly sorted breccia containing clast of nodular geyserite (*white square outline*); Kohuamuri deposit. **d** Nodular, pseudocolumnar geyserite from Yellowstone National Park (YNP) (USA), forming at high temperatures (>75 °C) proximal to a vent. **e** Geyserite pisoids ('beads') from the Kaitoke deposit. **f** Holocene geyserite collected proximal to a recently extinct vent at Geyser Valley, Wairakei, TVZ, New Zealand, indicating a similar texture to that found in (**e**). **g** Microtexture of geyserite spicules forming perpendicular to bedding, plane polarised light; Kohuamuri deposit. **h** Thin section (plane polarised light) of modern spicular geyserite from YNP, exhibiting a similar size and morphology of textures compared to the Kohuamuri deposit in (**g**). **i** Cut slab from the Kohuamuri deposit of finely laminated macrofacies showing low amplitude wavy lamination. **j** Photograph of cut slab of finely laminated macrofacies associated with geyserite (not shown), from high temperature sinter of the Te Kopia steaming landslide deposit, TVZ, New Zealand

common (Fig. 6g), and clotted fabrics are associated with distal apron settings in the Holocene Umukuri sinter, TVZ (Campbell et al. 2001).

In the inferred distal sinter apron facies at Kohuamuri, preservation in fine-grained quartz is rather patchy (e.g. Fig. 6a). For example, in Kohuamuri palisade fabrics, centimetre-scale bands of well-preserved, densely packed, vertical filaments commonly alternate with horizons of poorly preserved filaments (Fig. 6h), possibly reflecting variations in original porosity within laminae, differentially preserved by secondary silica infill. Alternatively, this depositional stacking pattern (filament-rich versus filament-poor, solid silica bands) could have been controlled by a 'pulse-pause' style of sheet flow across terrace areas, which may have shifted from continuous, to gradually or abruptly declining, or to locally ceasing altogether owing

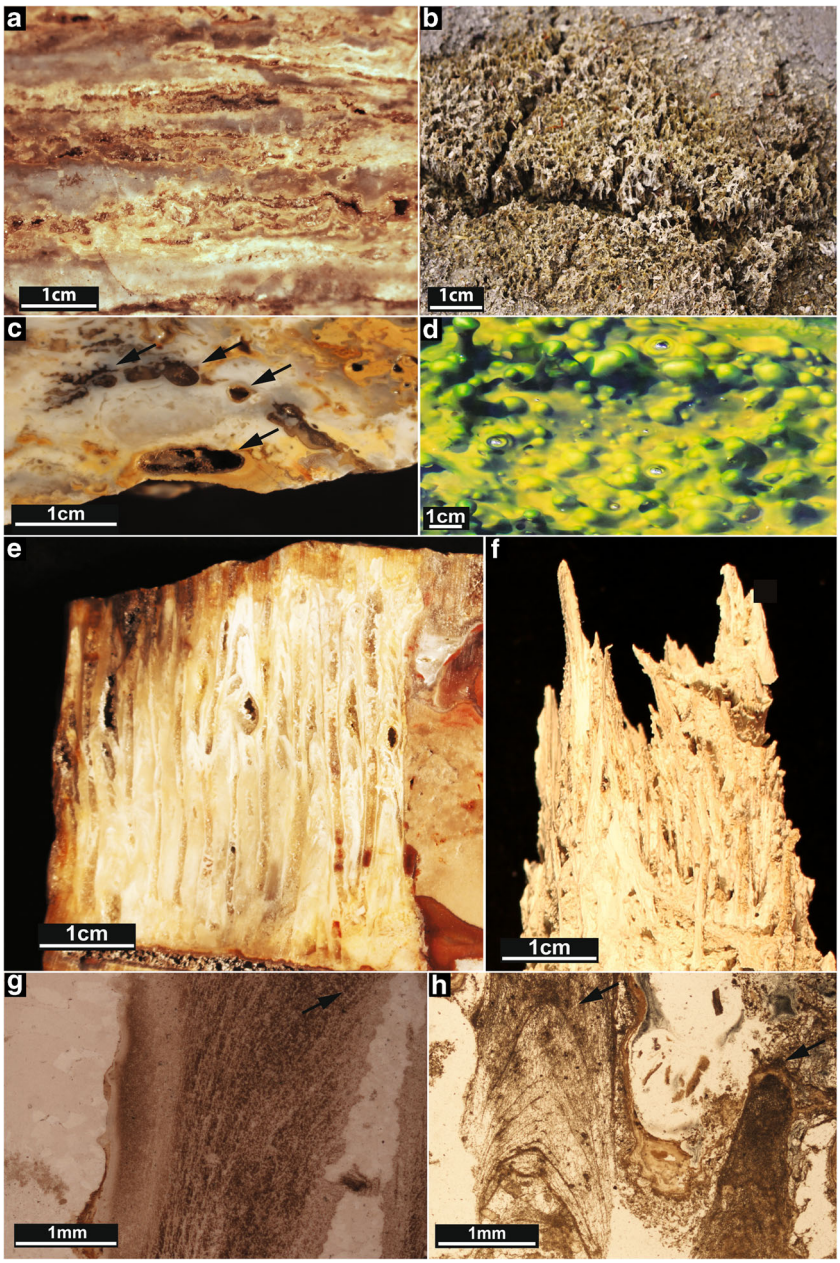

Fig. 5 Mid-apron sinter facies at Kohuamuri compared to modern examples. **a** Cut slab of network facies, comprising white webbed silica; Kohuamuri deposit. **b** Modern-day network facies forming on the dried margin of a hot pool at Tokaanu, TVZ. **c** Cut sinter slab showing a wavy laminated to low amplitude conical tufted fabric containing lenticular voids (*arrows*) produced by bubbles trapped within the Kohuamuri sinter deposit. **d** Modern-day example of 'bubble mat' forming within microbial mats at Waipahihi, TVZ. **e** Kohuamuri conical tufted facies showing individual tufts up to 5 cm in length. **f** Modern conical tufted sample from Whakarewarewa showing individual tufts. **g** Tall, steeply conical, tufted sinter microtexture in plane polarised light showing fossilised, stringy, fine microbial filaments (*dark*) surrounded by microcrystalline euhedral quartz (*white*); Kohuamuri deposit. **h** Modern conical filaments (*dark*) with high primary porosity (i.e. no mineral cement in the clear [*white*] areas); Whakarewarewa

to channel switching, climatic conditions or episodic dormancy of a spring vent (Campbell et al. 2015a).

The locations of ten different textural types—nodular/spicular/pisoidal geyserite, finely laminated, network, bubble mat, conical tufted, palisade, plant-rich and clotted—from in situ samples reveal the palaeo-flow direction and palaeotemperature gradient at Kohuamuri (Fig. 10). Facies mapping shows that vent fluids were expelled proximal to sites 9, 10 and 2. Furthermore, it can be inferred that the geothermal fluid expelled near site 10 flowed westwards to form a cool but thermally influenced marshland at site 5. The only in situ, moderate temperature, mid-apron texture was network fabric at site 11, 5 m to the southeast of the deduced vent area. This may have been an ephemeral pool that formed and then dried. It is also inferred that the extensive bedded sinter bluffs were produced in a mid- to distal apron setting, although textural details are obscured owing to strong diagenetic recrystallisation.

Mineralogy

Bulk XRD analysis utilising powdered representative samples showed the Kohuamuri sinter to be composed predominantly of quartz with no silica polymorphs. Optical microscopy verified that rims of some vugs contain chalcedony. Examination of these chalcedonic horizons using confocal Raman microscopy indicated the presence of minor moganite (<5 %), a distinctive monoclinic polymorph of silica. The chalcedony

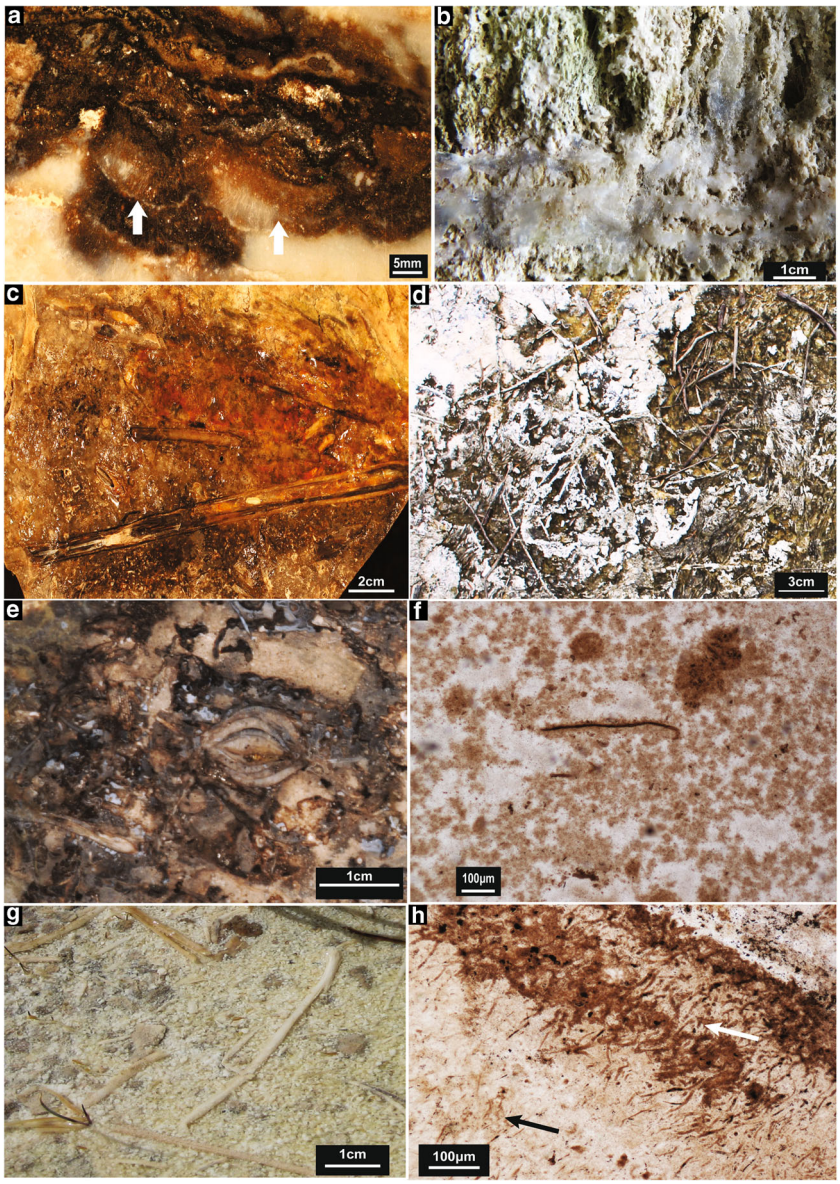

Fig. 6 Distal apron sinter facies and silicified, thermally influenced marsh fabrics at Kohuamuri compared to Holocene examples. **a** Preserved palisade filaments (*arrows*) within the Kohuamuri deposit. **b** Modern palisade fabric comprising pillar structures perpendicular to wavy lamination; Orakei Korako, TVZ. **c** Large fossilised reeds in plant-rich sinter from the Kohuamuri deposit. **d** Plant material silicified today on the distal apron at Tokaanu, TVZ. **e** Cut slab of clotted fabric (dark, irregular layers) forming around plant remains; black sinter north of Kohuamuri Stream. **f** Thin section image of dark clotted microtextures encrusting darker filaments at Kohuamuri in plane polarised light. **g** Modern-day example of clotted fabric of fluffy microbial encrustations (buff greenish colour) forming within a thermally influenced marsh, Yellowstone National Park. **h** Preservation of filaments within wavy palisade fabric in plane polarised light with examples of well-preserved filaments (*white arrow*) and poorly preserved filaments (*black arrow*); Kohuamuri deposit

silica polymorph is believed to be a transition phase that forms between opal-C and quartz, and which typically obliterates primary textures (Rodgers et al. 2004).

At a late stage in the Kohuamuri paragenetic sequence, hydrothermal minerals deposited within vugs of several sinter textures, as revealed under plane- and cross-polarised light, and using SEM (Fig. 7). These include adularia, mordenite, iron oxides, jarosite, sulphur and pyrite which can form at relatively low temperatures in epithermal environments. For example, mordenite and jarosite develop at <120 °C (Browne 1984).

The poorly sorted clasts within the hydrothermal breccia include volcanic materials, such as primary quartz crystals, plagioclase, tuffaceous sediments, as well as hydrothermal minerals (Fig. 7e–h). Plagioclase was partially to completely altered to illite (Fig. 7g); adularia also was partially altered to illite (Fig. 7h). The significance of these mineral occurrences is evaluated further in the discussion section below.

Trace element concentrations

Analysis detected most of the 21 targeted elements, with the exception of Ca, Mg and Se. The accepted pathfinder elements of Au, Ag, As and Sb in the Kohuamuri sinter showed typical signatures within the same range as other fossilised hot spring deposits (Table 2). The concentration of trace elements varied greatly (Supplementary Table 1), and while this may have had a primary cause, the differences also could have been influenced by spatially variable intensity of diagenesis, as observed by patchy preservation quality of filaments within the outcrops. Trace

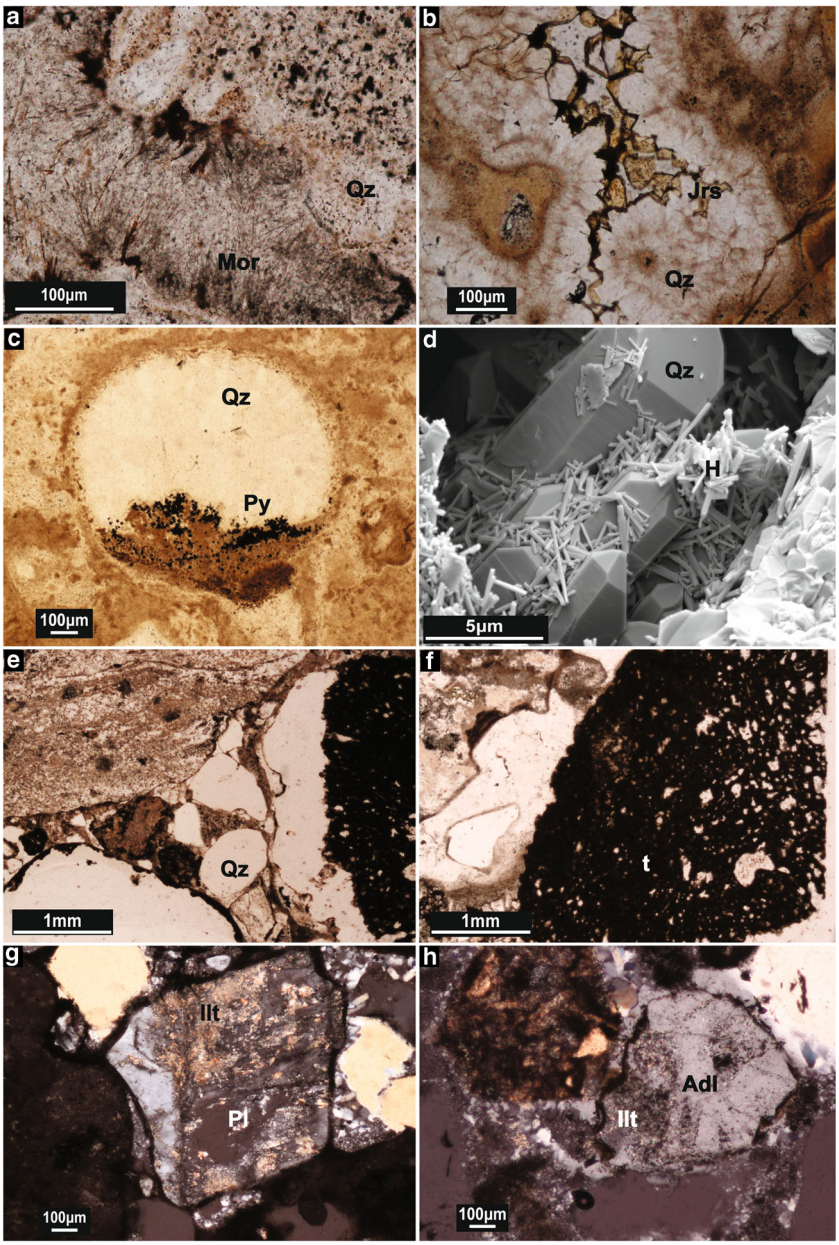

Fig. 7 Mineral microtextures within vugs of the Kohuamuri deposit. **a** Mordenite (*Mor*) entombed in euhedral quartz (*Qz*). **b** Jarosite (*Jrs*, *yellow*) in high relief, post-dating quartz microcrystal formation. **c** Thin section of pyrite (*Py*, *black*) in geopetals, followed by quartz (*Qz*) microcrystal fill of vug. **d** SEM image of halloysite (**h**) growing on quartz microcrystals (*Qz*). **e** Grain of primary quartz (*Qz*) formed in a volcanic setting. **f** Dark, tuffaceous material (*t*) formed in a volcanic environment. **g** Clast of grey twinned plagioclase (*Pl*) altering to highly birefringent illite clay (*Ilt*). **h** Grey clast showing alteration of adularia to illite (*Ilt*) with adularia (*Adl*)

element concentrations are plotted in Fig. 8 along an inferred palaeo-flow path deduced from textural analysis in order to evaluate whether enrichment changed with distance away from the implied vent area, along the interpreted temperature gradient. Relatively high concentrations were measured for all elements for textures associated with vent and proximal slope facies, and the lowest values were detected in sinter facies of the distal sinter apron (Fig. 8). Furthermore, sinter facies analysed for trace elements from in situ outcrops and float blocks show a trend of decreasing enrichment from high- to low-temperature facies with respect to Au, Ag, As, Ba, Hg, Mo, S and Tl. These trends are skewed by the mixed mineralogy of the poorly sorted breccia. Excluding the breccia samples reveals that Au, Ba, Hg, Li, S and Tl were highest in concentration in spicular geyserite, which forms in the splash zone of geysers and vents. The proximal facies of finely laminated textures contained the most Ag, Fe, Mn, Wo and Zn. By contrast, the lowest concentrations of Ag, Au, As, Ba, Li and Mo occur within the plant-rich facies formed in distal sinter apron areas. Elemental associations indicate that certain metals display a positive correlation within the Kohuamuri deposit, such as Au and Ag; As and Au; and Ag, Ba, Cu, Hg, Pb, S, Tl and As (Fig. 9). Strong correlations also were noted with Ba, Hg, Pb and Sb. Antimony has a moderately positive correlation with Au and Ag.

Table 2 Comparative trace element concentrations (ppm) in the Kohuamuri sinter and other fossilised hot-spring deposits elsewhere; modified from Guido et al. (2010)

Location	Age	Description	Au	Ag	As	Sb	Reference
Kohuamuri, New Zealand	Miocene–Pliocene	Sinter	0.001–0.119 ($n=18$)	0.05–10.1 ($n=18$)	2–344 ($n=18$)	1.36–96.7 ($n=18$)	This paper
San Agustin, Argentina	Jurassic	Sinter	0.001–0.003 ($n=3$)	<0.05–0.22 ($n=3$)	<0.1–78.8 ($n=3$)	0.48–3.03 ($n=3$)	Guido et al. 2010
Queensland, Australia	Devonian–Carboniferous	Sinter	<0.008–0.01 ($n=10$)	<1 ($n=10$)	<2–50 ($n=10$)	4–13 ($n=10$)	Cunneen and Sillitoe 1989
Rhynie, Scotland	Devonian	Chert	0.05–0.18 ($n=4$)	<2 ($n=4$)	15–66 ($n=4$)	<5–22 ($n=4$)	Rice and Trewin 1988

Discussion

The identified ancient Kohuamuri deposit textures are similar to those now forming in active hot springs, as inferred from macro- and micro-scale comparisons (e.g. Figs. 4, 5 and 6). This enabled interpretation of a palaeo-thermal gradient (100 °C–ambient) of the discharging fluids. It also allowed the reconstruction of five facies assemblages containing 12 textural types within a proximal, middle and distal sinter apron setting (Table 1). Spatial facies relationships were mapped to delineate the inferred paleo-flow direction and paleo-temperatures of the in situ deposit (Fig. 10). Thus, palaeo-geothermal fluids were expelled proximal to site 10, possibly from a single vent.

The vertical extent of bedded sinter, more than 10 m thick in some places, suggests that the Kohuamuri sinter was a relatively long-lived system (Guido and Campbell 2014). The 90 m vertical extent of the deposit also suggests that it had a high hydraulic head, as the deposit is both vertically and laterally extensive and shows no evidence of post-depositional faulting or uplift. The textures also suggest high volumes of water discharged from the system. For example, the large conical tufts (Fig. 5e) required maintenance of relatively deep pools of moderate temperature (40–60 °C) in which to form, similar to the large conical tufted features in the Jurassic Claudia palaeo-geothermal system of the Deseado Massif epithermal province, Patagonia, Argentina (Guido and Campbell 2014).

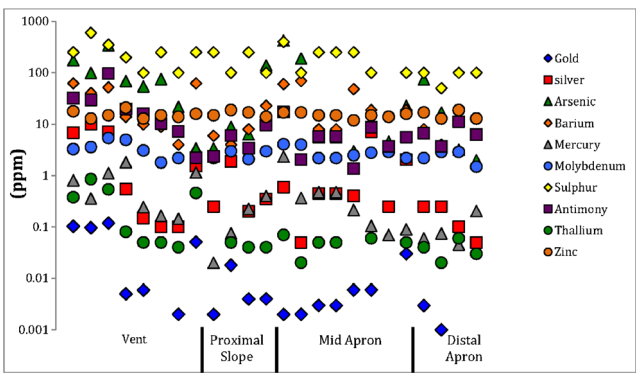

Fig. 8 Trace element concentrations of Au, Ag, As, Ba, Hg, Md, S, Sb, Th and Zn compared to distance from the inferred vent position at the Kohuamuri sinter based on textural analysis (see Fig. 10)

Based on textural, biotic and compositional evidence, the Kohuamuri siliceous sinter is inferred to have developed from near-neutral pH alkali chloride waters (Henley and Ellis 1983; Cady and Farmer 1996; Campbell et al. 2001, 2015a, b; Guido and Campbell 2011; Lynne 2012; Drake et al. 2014). Such sinters are far more common in the geological record than deposits of much thinner (millimetres to centimetres thick) silica residue or sinter formed in acid-sulphate-chloride waters, which are superficially similar in appearance but have quite different origins as products of acidic waters (Rodgers et al. 2004; Schinteie et al. 2007). The Kohuamuri sinter is composed predominantly of silica that preserves textures similar to those associated with organisms living in near-neutral pH alkali chloride waters today (Cady and Farmer 1996; Guido and Campbell 2011; Handley and Campbell 2011; Lynne 2012). The enrichment of Au, Ag, As and Sb in the Kohuamuri sinter is associated with near-neutral alkali chloride waters in active geothermal systems (Henley and Ellis 1983; McKenzie et al. 2001; Pope et al. 2005) and also occurs in the fossilised sinter of the Rhynie cherts, Scotland (Rice et al. 1995). Hydrothermal minerals can develop at relatively low temperatures in epithermal environments, e.g. mordenite and jarosite form at <120 °C, and the zeolite mordenite in the Kohuamuri sinter further implies that the deposit originated from thermal waters of near-neutral pH (Browne 1984). The presence of iron oxides and hydroxides, associated with pyrite and jarosite, are likely products of late oxidation produced either by weathering or overprinting by steam heated acid condensate as thermal activity waned (Browne 1991; Rogers et al. 2002).

It is not clear whether the Kohuamuri and Kaitoke deposits formed contemporaneously as part of the same geothermal system, as no detailed age information is available. Sinters can build up over large areas, such as at the Wai-O-Tapu field, TVZ or the Clepsydra/Fountain/Red geyser group and its extensive sinter apron at Fountain Paint Pots, Lower Geyser Basin, YNP. In addition, the focus of activity can laterally

migrate over time due to sealing of subsurface 'plumbing' and changes in hydrologic flow paths produced by micro-earthquakes and fluctuations in the water table (Rowland and Simmons 2012) such that age relationships may neither be straightforward nor stratigraphic (e.g. Drake et al. 2014).

Entrained clasts from the inferred hydrothermal eruption breccia in the Kohuamuri deposit provide useful mineralogical information about the palaeo-hydrothermal system at depth (Browne and Lawless 2001). For example, plagioclase alteration to illite is evident (Fig. 7g) and occurs within active geothermal systems at temperatures >210 °C (Browne 1984; Junfeng and Browne 2000). Illite occurs within epithermal deposits such as at Kohuamuri, partially replacing plagioclase and adularia (Fig. 7g, h), and may be found close to ore-producing quartz veins (Simmons et al. 2005; Tosdal et al. 2009), such as in the Golden Cross Au-Ag epithermal deposit of the Hauraki Goldfield (Simpson and Mauk 2011). Adularia indicates the presence of highly permeable rocks hosting thermal waters of near-neutral pH that had boiled (Browne and Ellis 1970; Simmons and Browne 2000).

A focus on textural analysis, such as in this study, enables differentiation of sinters from other siliceous palaeo-surface features (e.g. silicified lake sediments, silicified volcanic rocks, pseudosinters or silicified travertines, water table fluctuations infusing silica into sediments), which may lead to

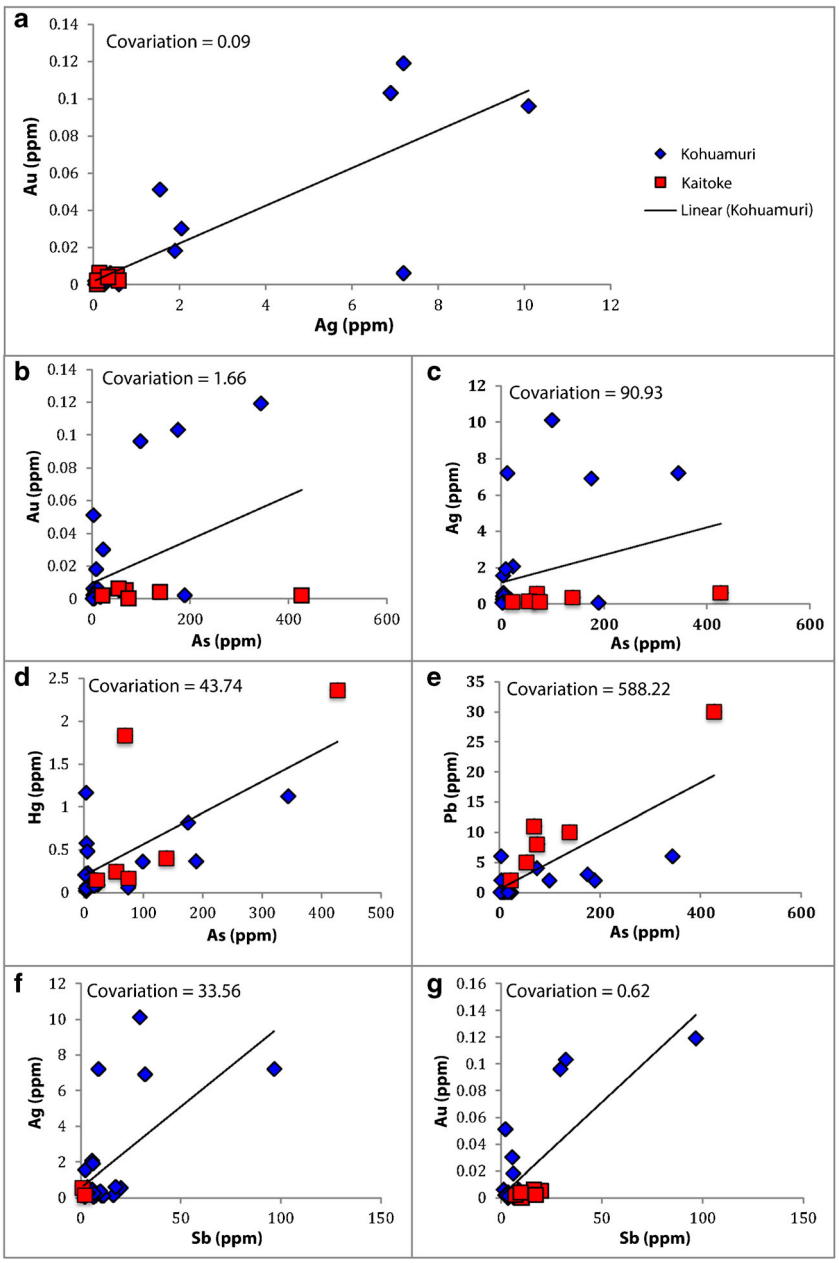

Fig. 9 Graphs showing positive correlation between certain elements within the Kohuamuri and Kaitoke sinter deposits, with covariation values. **a** Au vs. Ag; **b** Au vs. As; **c** Ag vs. As; **d** Hg vs. As; **e** Pb vs. As; **f** Ag vs. Sb; **g** Au vs. As

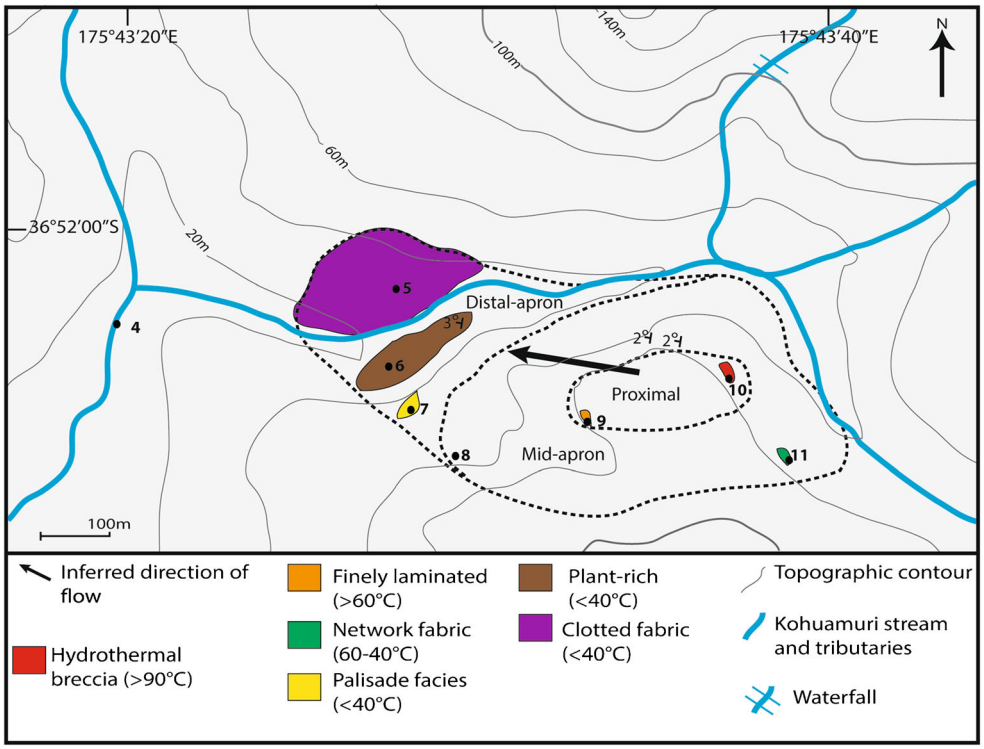

Fig. 10 Map showing the spatial relationship of in situ lithofacies for the Kohuamuri sinter. An *arrow* indicates the predominant direction of geothermal fluid flow during sinter formation. Inferred lithofacies associations also are outlined

misidentifications (Guido and Campbell 2011), such as has occurred within the CVZ (e.g. the Ohui 'sinter'; Brathwaite et al. 2001). Where hydrothermal breccias contain sinter clasts, such as at Kohuamuri and Onemana (Stevens and Boswell 2006), and if they also show anomalous metal enrichment, it is necessary to determine if the metals are part of the brecciation event or were incorporated within the sinter clasts prior to brecciation. Spatially detailed studies with good outcrop and/or core coverage are required to determine the specific relationships between metal enrichment in surface sinters and breccias with respect to any ore deposition at depth. Furthermore, the metal enrichment in some sinters may be controlled by factors other than proximity to the vent, which also must be taken into consideration in any exploration study involving sinters. For instance, in modern sinters, metals are concentrated within certain stromatolitic facies, owing to the physiochemical influence of microorganisms (Seward and Sheppard 1986; McKenzie et al. 2001; Mountain et al. 2003). This is due to EPS associated with microbes providing highly reactive sorption surfaces for nucleation of inorganic phases, such as heavy metals (McKenzie et al. 2001). The magnitude of enrichment also may vary in individual sinter deposits owing to local temperature of silica precipitation, the original composition of the geothermal fluid (Ewers 1991) and the intensity of late silica overprinting or later diagenesis (Guido and Campbell 2009, 2011).

The Kohuamuri sinter contains above ambient concentrations of Au, Ag, As, Pb, Hg, Mo and Sb, as occur also in some modern and fossilised geothermal deposits (Henley and Ellis 1983; McKenzie et al. 2001; Groves 2007), and is similar to that reported from sinter clasts associated with the inferred hydrothermal breccia of the Onemana deposit in the Hauraki Goldfield (Stevens and Boswell 2006). At Kohuamuri, the average detected values of trace elements typical of epithermal mineralisation are within the range of those reported from commercial mining operations of the Moonlight sinter (Drummond Basin, Australia; Groves 2007), Red Butte sinter (Oregon; Zimmerman and Larson 1994) and McLaughlin sinter (California; Sherlock et al. 1995). The concentrations of these elements in the Kohuamuri sinter also are within the same range as those measured in the distal alteration halo of the Empire Vein, Golden Cross, Waihi, CVZ (Simpson and Mauk 2011). At Kohuamuri, a wide range in values was measured (>4 orders of magnitude), similar to modern active and extinct sinters at Wai-O-Tapu, TVZ (Wilson et al. 2012), and the Rhynie cherts, Scotland (Trewin 1993). A depletion in dissolved metals in thermal waters with distance from a vent was reported for Sb at Wai-O-Tapu, Champagne Pool, TVZ, where its concentration in the discharge channel dropped from approximately 150 μg/l at 100 m from the pool to below detection at 300 m distance (Pope et al. 2004). This suggests that the metals incorporated within some sinters, including Kohuamuri, may have been concentrated during sinter formation.

The positive correlation of certain trace element associations (Fig. 9) at Kohuamuri is similar to that observed today at Wai-O-Tapu (Pope et al. 2005) and Broadlands-Ohaaki (Simmons and Browne 2000), where this relationship is

believed to be due to co-precipitation with colloidal sulphides containing these elements (Simmons et al. 2005). Other studies suggest that trace elements do not always precipitate in sulphides but may encrust opal-A in sinter deposits (Jones and Renaut 2003). The correlation of these metals within the Kohuamuri sinter suggests that sulphides may have been present within the epithermal-geothermal system. This is important because the precipitation of sulphides is required to form epithermal ore deposits at depth (Simmons et al. 2005), and such a positive correlation has been observed in other epithermal deposits in the Coromandel region, such as at Golden Cross, Hauraki Goldfield (Simpson and Mauk 2011).

This study is the first to analyse the trace element geochemistry of an ancient sinter across a suite of textures indicative of vent to marsh environments. The identified palaeo-geothermal gradient in the sinter fabrics shows a trend of increased metal concentrations (Au, Ag, As, Ba, Hg, Mo, S, Tl) with proximity to the vent, providing evidence that the fluid forming the sinter contained anomalous levels of precious metals rather than the enrichment being a product of late-stage hydrothermal or burial fluids. In the latter case, we would expect the trace element distribution to be more irregularly distributed throughout the sinter rather than relatively higher in the near-vent facies. In comparison, trace elemental studies of other sinters elsewhere (Table 2) have not listed environmental or diagenetic textures of sinter in relation to trace element distributions, which has introduced uncertainty in the use of siliceous hot spring deposits as indicators of mineralisation at depth. Thus, it is essential to establish a paragenetic framework for each sinter deposit in order to decipher the fluid history of a given palaeo-geothermal system. The Kohuamuri results illustrate the importance of identifying primary and diagenetic textures to determine at which point in the lifetime of an epithermal system metals may have precipitated or whether they migrated into it from elsewhere, such as in a late-stage hydrothermal overprinting event (McLaughlin deposit; Sherlock et al. 1995). A textural-geochemical approach of reconstructing the relative spatial and temporal distribution of trace metal concentrations with respect to the surface hot-spring discharge gradient opens up new possibilities for sinters to be effectively utilised as vectors for epithermal mineralisation.

Conclusions

The Kohuamuri sinter, enriched in precious metals (Au, Ag) and pathfinder elements (As, Sb) mineralized as sulphides, represents an ancient near-neutral pH alkali chloride hot-spring deposit where fluids at ≤100 °C were expelled through a vent located at the land surface, derived from reservoir temperatures >210 °C in which boiling appears to have occurred. This study shows how analysis of textures, mineralogy and element concentrations of siliceous sinter deposits may allow recognition of thermal fluid flow sites from reservoir to the land surface by recognising discharge areas in temperature-dependent palaeoenvironmental gradients. These data, which may be extracted from modern and fossil sinter, have implications for epithermal exploration as they provide a low-impact and relatively simple method for targeting possible sites of mineralisation at depth. This method could be used throughout the Hauraki Goldfield, and it has proven useful in exploration of other goldfields elsewhere.

Acknowledgments AH's research was funded by the Institute of Mining and Metallurgy New Zealand Branch—Education Endowment Trust Scholarship, Newmont Waihi Gold and The University of Auckland Geology Centennial Award. KAC and PRLB received financial support for reconnaissance field work from the Royal Society of New Zealand's Marsden Fund. During manuscript preparation, AH, KAC, and JVR were funded by the Ministry for Business, Innovation and Employment (MBIE), onshore minerals project, 'Mineral exploration models to drive discovery and reduce exploration risk'. Technical assistance was provided by Ben Durrant, Dr Michel Nieuwoudt, John Wilmshurst, Patrick Conor, John Robertson and Louise Cotterall. The manuscript was improved by reviews from R.L. Brathwaite and S.F. Simmons.

References

Adams CJ, Graham IJ, Seward D, Skinner DNB, Moore PR (1994) Geochronological and geochemical evolution of late Cenozoic volcanism in the Coromandel Peninsula, New Zealand. N Z J Geol Geophys 37(3):359–379

Bell JM, Fraser C (1912) The geology of the Waihi-Tairua subdivision, Hauraki division, Auckland. N Z Geol Survey Bull 15:192

Booden MA, Smith IEM, Black PM, Mauk JL (2012) Geochemistry of the Early Miocene volcanic succession of Northland, New Zealand, and implications for the evolution of subduction in the Southwest Pacific. J Volcanol Geotherm Res 199(1–2):25–37

Brathwaite RL, Cargill HJ, Christie AB, Swain A (2001) Lithological and spatial controls on the distribution of quartz veins in andesite- and rhyolite-hosted epithermal Au–Ag deposits of the Hauraki Goldfield, New Zealand. Miner Deposita 36(1):1–12

Braunstein D, Lowe DR (2001) Relationship between spring and geyser activity and the deposition and morphology of high temperature (>73°C) siliceous sinter, Yellowstone National Park, Wyoming, U.S.A. J Sediment Res 71:747–763

Briggs RM, Houghton BF, McWilliams M, Wilson CJN (2005) $^{40}Ar/^{39}Ar$ ages of silicic volcanic rocks in the Tauranga-Kaimai area, New Zealand: dating the transition between volcanism in the Coromandel Arc and the Taupo Volcanic Zone. N Z J Geol Geophys 43(3):459–469

Browne PRL (1984) Lectures on geothermal geology and petrology. UNU Geothermal Training Programme, National Energy Authority, Reykjavik

Browne PRL (1991) Mineralogical guides to interpreting the shallow paleohydrology of epithermal mineral depositing environments. In: 13th New Zealand Geothermal Workshop. New Zealand Geothermal Institute, Auckland, p 263–169

Browne PRL, Ellis AJ (1970) The Ohaaki-Broadlands hydrothermal area, New Zealand; mineralogy and related geochemistry. Am J Sci 269: 97–131

Browne PRL, Lawless JV (2001) Characteristics of hydrothermal eruptions, with examples from New Zealand and elsewhere. Earth-Sci Rev 52:299–331

Buchanan LJ (1981) Precious metal deposits associated with volcanic environments in the Southwest. Ariz Geol Soc Digest 14:237–262

Cady SL, Farmer JD (1996) Fossilization processes in siliceous thermal springs: trends in preservation along thermal gradients. Ciba Found Symp 202:150–153

Campbell KA, Sannazzaro K, Rodgers KA, Herdianita NR, Browne PRL (2001) Sedimentary facies and mineralogy of the late Pleistocene Umukuri silica sinter, Taupo Volcanic Zone, New Zealand. J Sediment Res 71:727–746

Campbell KA, Lynne BY, Handley KM, Jordan S, Farmer JD, Guido DM, Foucher F, Turner S, Perry RS (2015a) Tracing biosignature preservation of geothermally silicified microbial textures into the geological record. Astrobiology 15(10):858–882

Campbell KA, Guido GM, Gautret P, Foucher F, Ramboz C, Westall F (2015b) Geyserite in hot-spring siliceous sinter: window on Earth's hottest terrestrial (paleo)environment and its extreme life. Earth-Sci Rev 148:44–64

Channing A, Edwards D, Sturtevant S (2004) A geothermally influenced wetland containing unconsolidated geochemical sediments. Can J Earth Sci 41:809–827

Christie AB, Simpson MP, Brathwaite RL, Mauk JL, Simmons SF (2007) Epithermal Au-Ag and related deposits of the Hauraki Goldfield, Coromandel Volcanic Zone, New Zealand. Econ Geol 102:785–816

Cunneen R, Sillitoe RH (1989) Paleozoic hot spring sinter in the Drummond Basin, Queensland, Australia. Econ Geol 84:135–142

Drake BD, Campbell KA, Rowland JV, Guido DM, Browne PRL, Rae A (2014) Evolution of a dynamic paleo-hydrothermal system at Mangatete, Taupo Volcanic Zone, New Zealand. J Volcanol Geotherm Res 282:19–35

Ewers GR (1991) Oxygen isotopes and the recognition of siliceous sinters in epithermal ore deposits. Econ Geol 86:173–178

Fournier RO (1985) Yellowstone magmatic-hydrothermal system, U.S.A. In: International symposium on geothermal energy; International volume., pp 319–327

Fournier RO, Rowe JJ (1966) Estimation of underground temperatures from the silica content of water from hot springs and wet-steam wells. Am J Sci 264:685–697

Fraser C, Adams JH (1907) The geology of the Coromandel Subdivision, Hauraki, Auckland. N Z Geol Surv Bull 4:156

Groves SR (2007) The Geology and genesis of the Moonlight Prospect, Pajingo Epithermal System, Northland Queensland: an investigation of a high-level, low sulfidation epithermal system. MSc Economic Geology (University of Tasmania), 145 pp

Guido DM, Campbell KA (2009) Jurassic hot-spring activity in a fluvial setting at La Marciana, Patagonia, Argentina. Geol Mag 146:617–622

Guido DM, Campbell KA (2011) Jurassic hot spring deposits of the Deseado Massif (Patagonia, Argentina): characteristics and controls on regional distribution. J Volcanol Geotherm Res 203:35–47

Guido DM, Campbell KA (2014) A large and complete Jurassic geothermal field at Claudia, Deseado Massif, Santa Cruz, Argentina. J Volcanol Geotherm Res 275:61–70

Handley KM, Campbell KA (2011) Character, analysis and preservation of biogenicity in terrestrial siliceous stromatolites fromgeothermal settings. In: Tewari VC, Seckbach J (eds) STROMATOLITES: interaction of microbes with sediments, cellular origin. Life in Extreme Habitats and Astrobiology 18, pp. 359–381. http://dx.doi.org/10.1007/978-94-007-0397-1_16

Guido DM, Channing A, Campbell KA, Zamuner A (2010) Jurassic geothermal landscapes and fossil ecosystems at San Agustín, Patagonia, Argentina. J Geol Soc Lond 167(1):11–20

Hedenquist JW, Henley RW (1985) Hydrothermal eruptions in the Waiotapu geothermal system, New Zealand: their origin, associated breccias, and relation to precious metal mineralization. Econ Geol 80:1640–1668

Henley RW, Ellis AJ (1983) Geothermal systems ancient and modern: a geochemical review. Earth-Sci Rev 19:1–50

Herdianita NR, Rodgers KA, Browne PRL (2000) Routine instrumental procedures to characterise the mineralogy of modern and ancient silica sinters. Geothermics 29:65–81

Hinman NW, Lindstrom RF (1996) Seasonal changes in silica deposition in hot spring systems. Chem Geol 132(1–4):237–246

Jones B, Renaut RW (2003) Hot spring and geyser sinters: the integrated product of precipitation, replacement, and deposition. Can J Earth Sci 40:1549–1569

Jones B, Renaut RW, Jones B, Renaut RW et al. (2011) Hot springs and geysers. In: Reitner J, Thiel V (eds) Encyclopedia of Geobiology. Springer, pp 447–451

Junfeng J, Browne PRL (2000) Relationship between illite crystallinity and temperature in active geothermal systems of New Zealand. Clay Clay Miner 48:139–144

King PR (2000) Tectonic reconstruction of New Zealand: 40 Ma to the present. N Z J Geol Geophys 43:611–638

Lowe DR, Braunstein D (2003) Microstructure of high temperature (>73°C) siliceous sinter depositing around hot springs and geysers, Yellowstone National Park: the role of biological and abiological processes in sedimentation. Can J Earth Sci 40:1611–1642

Lynne BY (2012) Mapping vent to distal-apron hot spring paleo-flow pathways using siliceous sinter architecture. Geothermics 43:3–24

Lynne BY, Campbell KA, Moore J, Browne PRL (2008) Origin and evolution of the Steamboat Springs siliceous sinter deposit, Nevada, U.S.A. Sediment Geol 210(3–4):111–131

Mauk JL, Hall CM, Chesley JT, Barra F (2011) Punctuated evolution of a large epithermal province: the Hauraki Goldfield, New Zealand. Econ Geol 106:921–943

McKay A (1897) Report on the geology of The Cape Colville Peninsula. In: Appendix to the Journals of the House of Representatives of New Zealand, 1897, vol C-9. Government Printers, New Zealand, pp 1–75

McKenzie EJ, Brown KL, Cady SL, Campbell KA (2001) Trace metal chemistry and silicification of microorganisms in geothermal sinter, Taupo Volcanic Zone, New Zealand. Geothermics 30:483–502

Mountain BW, Benning LG, Jackson S (2003) Metalliferous stromatolites from New Zealand hot springs. Goldschmidt Conference, Kurashiki, Geochim Cosmochim Acta 67/18, A309 (abstr)

Pope JG, McConchie DM, Clark MD, Brown KL (2004) Diurnal variations in the chemistry of geothermal fluids after discharge, Champagne Pool, Waiotapu, New Zealand. Chem Geol 203:253–272

Pope JG, Brown KL, McConchie DM (2005) Gold concentrations in springs at Waiotapu, New Zealand: implications for precious metal deposition in geothermal systems. Econ Geol 100:677–687

Rattenbury MS, Partington GA (2003) Prospectivity models and GIS data for the exploration of epithermal gold mineralization in New Zealand. Crown Minerals, New Zealand Petroleum and Minerals and Institute of Geological and Nuclear Sciences (CD-ROM)

Rice CM, Trewin NH (1988) A Lower Devonian gold-bearing hot-spring system, Rhynie, Scotland. In: Transactions of the Institution of Mining and Metallurgy Section B Applied Earth Science 97 (August) 1988., pp 141–144

Rice CM, Ashcroft WA, Batten DJ, Boyce AJ, Caulfield JBD, Fallick AE, Hole MJ, Jones E, Pearson MJ, Rodgers G, Saxton JM, Stuart FM, Trewin NH, Turner G (1995) A Devonian auriferous hot spring system, Rhynie, Scotland. J Geol Soc Lond 152:229–250

Rodgers KA, Browne PRL, Buddle TF, Cook KL, Greatrex RA, Hampton WA, Herdianita NR, Holland GR, Lynne BY, Martin R, Newton Z, Pastars D, Sannazarro KL, Teece CIA (2004) Silica phases in sinters and residues from geothermal fields of New Zealand. Earth-Sci Rev 66:1–61

Rogers KA, Cook KL, Browne PRL, Campbell KA (2002) The mineralogy, texture and significance of silica derived from alteration by

steam condensate in three New Zealand geothermal fields. Clay Miner 37:299–322

Rowland JV, Simmons SF (2012) Hydrologic, magmatic, and tectonic controls on hydrothermal flow, Taupo Volcanic Zone, New Zealand: implications for the formation of epithermal vein deposits. Econ Geol 107:427–457

Schinteie R, Campbell KA, Browne PRL (2007) Microfacies of stromatolitic sinter from acid-sulphate-chloride springs at Parariki Stream, Rotokawa Geothermal Field, New Zealand. Palaeontol Electron 10(issue 1):4A–33A

Seebeck H, Nicol A, Giba M, Pettinga J, Walsh J (2014) Geometry of the subducting Pacific Plate since 20 Ma, Hikurangi margin, New Zealand. J Geol Soc Lond 171(1):131–143

Seward TM, Sheppard DS (1986) Waimangu geothermal field. In: Henley RW, Hedenquist JW, Roberts PJ (eds) Guide to active epithermal (geothermal) systems and precious metal deposits of New Zealand., pp 81–91, Gebruder Borntraeger, Berlin, Stuttgart Monograph Series of Mineral Deposits

Sherlock RL, Tosdal RM, Lehrman NJ, Graney JR, Losh S, Jowett EC, Kesler SE (1995) Origin of the McLaughlin Mine sheeted vein complex; metal zoning, fluid inclusion, and isotopic evidence. Econ Geol 90:2156–2181

Sillitoe RH (2015) Epithermal paleosurfaces. Miner Deposita 50(7):767–793

Sillitoe RH, Hedenquist JW (2003) Linkages between volcanotectonic settings, ore fluid compositions, and epithermal precious metal deposits. In Simmons SF and Graham IJ (eds) Volcanic, geothermal, and ore forming fluids: rulers and witnesses of processes within the Earth. Soc Econ Geol Spec Pub 10:315–343

Simmons SF, Browne PRL (2000) Hydrothermal minerals and precious metals in the Broadlands-Ohaaki Geothermal System: implications for understanding low-sulfidation epithermal environments. Econ Geol 95:971–999

Simmons SF, White NC, John DA (2005) Geological characteristics of epithermal and base metal deposits. In: Econ Geol 100th Anniversary Volume., pp 485–522

Simpson MP, Mauk JL (2011) Hydrothermal alteration and veins at the epithermal Au-Ag deposits and prospects of the Waitekauri Area, Hauraki Goldfield, New Zealand. Econ Geol 106:945–973

Skinner DNB (1986) Neogene volcanism of the Hauraki Volcanic Region. In: Smith IEM (ed) Cenozoic volcanism in New Zealand, vol 23., pp 21–47, The Royal Society of New Zealand Bulletin

Skinner DNB (1995) Geology of the Mercury Bay Area. Scale 1:50000. In: Institute of Geological & Nuclear Sciences geological map 17. 1 sheet + 56 p. Institute of Geological and Nuclear Sciences Limited, Lower Hutt

Stevens MR, Boswell GB (2006) Geology and exploration of the Onemana Au-Ag prospect, Whangamata, Hauraki Goldfield. In: Christie AB, Brathwaite RL (eds) Geology and exploration of New Zealand mineral deposits, AusIMM Monograph 25., pp 123–130

Tosdal RM, Dilles JH, Cooke DR (2009) From source to sinks in auriferous magmatic-hydrothermal porphyry and epithermal deposits. Elements 5:289–295

Trewin NH (1993) Depositional environment and preservation of biota in the Lower Devonian hot-springs of Rhynie, Aberdeenshire, Scotland. Earth Environ Sci Trans R Soc Edinb 84:433–442

Walter MR (1976) Stromatolites. Elsevier Scientific Publishing Company, Amsterdam, p 261

Walter MR, Des Marais D, Farmer JD, Hinman NW (1996) Lithofacies and biofacies of mid-Paleozoic thermal spring deposits in the Drummond Basin, Queensland, Australia. Palaios 11:497–518

Walter MR, McLoughlin S, Drinnan AN, Farmer JD (1998) Palaeontology of Devonian thermal spring deposits, Drummond Basin, Australia. Alcheringa 22:285–314

White NC, Wood DG, Lee MC (1989) Epithermal sinters of Paleozoic age in north Queensland, Australia. Geology 17:718–722

Wilson CJN, Rowland JV (2015) The volcanic, magmatic and tectonic setting of the Taupo Volcanic Zone, New Zealand, reviewed from a geothermal perspective. Geothermics 59:168–187

Wilson N, Webster-Brown J, Brown KL (2012) The behaviour of antimony released from surface geothermal features in New Zealand. J Volcanol Geotherm Res 247–248:158–167

Zimmerman BS, Larson PB (1994) Epithermal gold mineralization in a fossilised hot spring system, Red Butte, Oregon. Econ Geol 89: 1983–2002